Single crystal growth of germanium – silicon alloys

ERCAN BALIKCI[*], AIDIN DARIO, HASAN OZGEN SICIM
Department of Mechanical Engineering, Bogazici University, Bebek 34342 Istanbul – Turkey

Germanium-silicon (Ge–Si) alloys enjoy a widespread interest because of their remarkable potential for optoelectronic, solar cell, thermoelectric power generation, and photodetector applications. Despite this obvious interest, Ge-Si crystal growth has difficulties. Ge-Si alloy system is extremely prone to segregation due to its thermo-physical properties. This prevents the growth of quality bulk crystals of Ge-Si, which are the basis for example for solar cells as wafers. A new bulk crystal growth technique called axial heat processing (AHP) is proposed to alleviate the adversities during Ge-Si single crystals. The technique makes use of an immersed baffle that spreads the heat over the growth interface, decreases the melt height, and divides melt into two regions. Several silicon doped germanium single crystals with 5 and 12 atomic percent concentration have been grown by the AHP method at 0.75 mm/h and 2 mm/h velocity with two different melt heights. Few Bridgman crystals have also been grown to set a base for a comparison between the crystals grown by the AHP and Bridgman techniques. The effect of the processing variables on the longitudinal and radial dopant distribution and single crystal quality is investigated. A new theoretical approach is also proposed to predict the solute redistribution and morphological stability in the grown crystals. The predictions of this new model are found to be superior when compared to those of Constitutional Supercooling (CS) and Mullins and Sekerka (MS) criteria.

1. Introduction

The silicon is a dominant semiconductor material in the microelectronic industry because of its cost and ease of processing. However, there are some applications where other advanced materials like Ge-Si supersede the silicon [1–3]. Ge-Si alloys allow engineering the band gap, energy band structure, and mobility that make these alloys versatile. There is a great range of applications where Ge-Si materials show superior performances, among which are the electronics, optoelectronics, and thermoelectric generators. For instance, Ge-Si thermoelectric materials have been successfully used in space in the SNAP-10A nuclear reactor, LES 8, LES 9, Voyager I, Voyager II, Galileo and Ulysses spacecrafts [3,4].

A large scale production of bulk Ge–Si alloys is needed to meet the immense demand of the industry and to reduce the cost of Ge-Si devices to a competitive level. Moreover, high quality bulk Ge–Si alloys are required to study the fundamental properties of these alloys [5]. Ge-Si alloys have been produced by the Chemical Vapor Deposition (CVD), melt growth, and hot press techniques. Disadvantages of the grain boundaries can be avoided by use of single crystals. An economical and high production rate of single crystals is only possible via melt growth methods. However, due to the thermo-physical properties of the Ge-Si alloys, production of these alloys is not easy by conventional techniques. A large difference in the melting temperatures (1211K for Ge and 1687K for Si), separation of the solidus and liquidus curves (160°C at 50%), density difference (5.51 g/cm3 for Ge and 2.53 g/cm3 for Si), segregation coefficient range (5.5 near pure Ge and 0.33 near pure Si), and difference in lattice

constants (5.43 Å for Ge and 5.66 Å for Si) make the solidification of the Ge-Si hard and very sensitive to the experimental parameters.
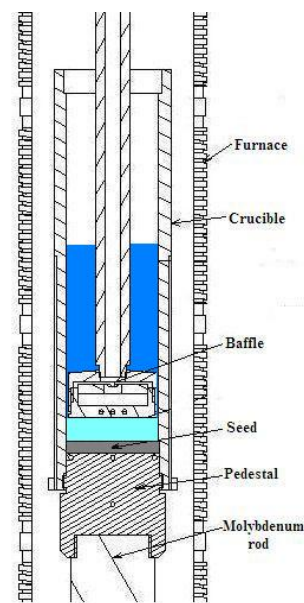

Fig. 1 Schematic of the AHP.

One of the important problems in this system is the strong segregation due to a large melting range. Of course, homogeneity in the melt grown bulk crystals is essential to ensure reproducibility of wafers with uniform electronic properties. Therefore, close control of the segregation in

the melt grown Ge-Si alloys is essential. However, conventional methods such as Czochralski (CZ), Vertical Bridgman (VB), and Floating Zone Melting (FZ) fall short of controlling the segregation since all these methods supply heat radially to the melt, so they create a high radial temperature gradient in the melt. Consequently, the radial temperature gradient creates a non-planar interface which makes the radial segregation inevitable.

A novel melt growth technique, dubbed Axial Heat Processing (AHP), has been developed [6] to combat problems encountered in conventional crystal growth techniques. A schematic of the technique is seen in Fig. 1.

The AHP method employs a baffle which may contain a heater. Alternatively, the baffle may be made of a highly conductive material. This baffle is submerged into the melt contained in a crucible to minimize the radial temperature gradient that results from the radial heating of the charge, a characteristic of all conventional methods. Minimizing the radial temperature gradient promotes formation of a planar interface. Moreover, the baffle separates the melt into two regions as upper (feeding region) and lower (solidification region). The melt flows through an annular gap between the baffle and the crucible, from the region above the baffle to the region below the baffle by relative motion of the crucible and baffle. The baffle reduces the melt height and the amount of the buoyancy driven convection. On the other hand, a forced flow is induced over the interface, the magnitude of which is controllable by adjusting dimensional parameters. A very similar method called Submerged Heater Method (SHM) was also developed by Ostrogorsky [7]. These techniques have successfully been used for production of several materials and for investigations on the effects of forced flow, natural convection, and interfacial kinetics on the morphological stability [8-17].

The aim of this study is to compare a conventional crystal growth technique (VB) and a recently developed one (AHP). Details of the study can be found in [18]. The objective of this paper is, in fact, to assess the influence of selected growth parameters, specific to the mentioned techniques, on the solute segregation and interface stability in Ge-Si semiconducting alloys.

2. Experimental

A single crystalline silicon disc (seed) with 40 mm diameter in [111] direction and germanium chunks were used to grow Ge-Si crystals. The germanium-silicon melt charge was obtained by dissolving the pure silicon seed into pure germanium chunks. The initial position of the solid/liquid (s/l) interface and the height of the seed that would be dissolved into the melt were estimated using the temperature profile of the furnace and the melting temperature data from the phase diagram. The seed was placed on top of a graphite pedestal which was then screw mounted to a graphite crucible so that the seed was fastened between the 0.5mm indent machined into the crucible and the top of the pedestal. This prevented floatation of the low density seed in the germanium melt. The germanium chunks were placed over the seed in the crucible. The crucible remained at its initial position for the estimated duration required for the silicon dissolution. For the Bridgman grown crystals, the crucible was pulled down immediately upon the end of the dissolution duration. Nevertheless, for the AHP grown crystals, at the end of this duration, the baffle was moved down until it touched the top of the seed and then pulled up again to mix the melt. Then once again the baffle was moved down to touch the seed, and this time the baffle was pulled up to a distance equal to the desired initial melt height. Then the crucible was pulled down to initiate the solidification process. The growth process was conducted under continuous flow of argon gas. The pressure of the argon gas inside the furnace was 1 atm above the atmospheric pressure. Axial temperature gradient on the crucible was 20°C/cm. Growth parameters of the crystals are presented in Table 1. The grown crystals were cold mounted before they were longitudinally bisected using a diamond saw. One longitudinal surface of each sample was prepared for characterization by the standard metallographic processes and investigated by an optical metal microscope. To reveal the growth microstructure, the polished surface was chemically etched with a $HF + H_2O_2 + H_2O$ solution (1:1:4 by volume) for 3 minutes. Compositional analysis was carried out by the Energy Dispersive X-ray Spectroscopy (EDS) technique. A grid layout was prepared for each sample separately according to the microstructural observations. Then EDS measurements were taken at each grid point.

Table 1. Samples and their Parameters

Sample	Initial Si content (at. %)	Initial melt height (mm)	Pulling speed (mm/h)	Experimental SC length (mm)	Predicted SC length (mm)	Gr x10^{-4}	U (mm/h)	Curvature depth (mm)
B12-40-2	13.56	44.00	2.00	4.10	-	18365	-	20.00
B12-50-075	10.00	53.00	0.75	11.00	-	38663	-	10.00
AHP12-10-2	12.38	10.00	2.00	4.00	6.00	49	81.01	8.00
AHP5-10-075	5.79	10.00	0.75	32.00	32.00	49	30.38	2.00

3. Results and discussions

After the growth, samples were found to be tightly squeezed in their crucibles. Thus, samples were pushed out of their crucibles using a hydraulic press very slowly. There was no visible defect on the surface of the samples, see Fig. 2. However, after the crystals were bisected by a diamond wafering disc, significant number of cracks was formed in the halved surfaces of the crystals, see Fig. 3. The reason for these cracks is traced to the grown-in dislocations initiated because of the lattice constant mismatch of silicon and germanium (5.43 Å vs 5.66 Å). One way to decrease the dislocations in the crystals may be the use of a seed with a concentration close to that of the growing crystal.

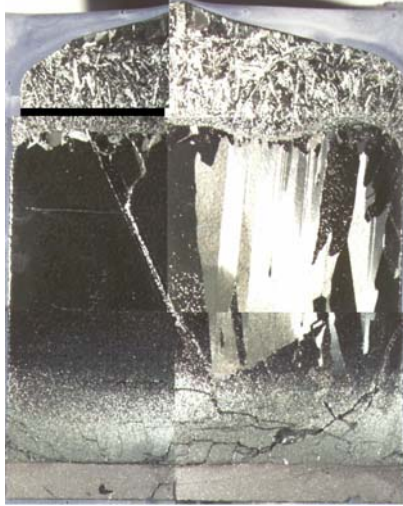*Fig. 2 A typical grown crystal*

Fig. 3 Micrograph of the etched half of AHPC5V075h10. Black line is due to a mismatch in mosaicing the micrographs.

Fig. 4 shows isoconcentration maps and axial solute distributions in the crystals. An isoconcentration map is constructed by a linear interpolation between the grid points at which the EDS data are obtained. In the maps, the horizontal axis shows the radial, the vertical axis shows the axial distance in a crystal, and each color represents the solute concentration at that point. Thus, an isoconcentration map is a 2-D visual presentation of segregation in grown crystals, which is influenced by the nature of flow in the melt.

The nature of the fluid flow during solidification influences the segregation and interface stability. The melts of the crystals grown in this study experience mixing due to the natural convection (buoyancy) or forced flow. The first one can be expected in both growth modes, but the latter one can only be present in AHP because of the relative motion of the crucible and the baffle. Type of the flow due to buoyancy can be assessed by the Grashof number that is the ratio of the Rayleigh number to the Prandtl number that gives the relative effect of buoyancy forces to the viscous forces as follows:

$$\text{Gr} = \frac{\text{Ra}}{\text{Pr}} = \frac{\text{Buoyancy Force}}{\text{Viscous Force}} = \frac{g \beta G_L h^4}{\upsilon^2} \qquad (1)$$

where g is the gravitational acceleration, ß the coefficient of volumetric expansion, G_L the thermal gradient in melt, h the melt height above the s/l interface, and ν the kinematic viscosity. The influence of the melt height is obvious from this formula. For Gr numbers less than 10^4, the viscous forces are supposed to be dominant and solute transport mode is diffusional. The Grashof number for each sample is calculated and provided in Table 1. The Grashof numbers show that reduction in the melt height dramatically reduces the buoyancy effect in the melt. Thus, for the AHP grown specimens, the Grashof number approaches the critical value of 10^4 under which the solute transport is assumed to be diffusional, meaning no disturbance in the liquid. However, a source of disturbance in the melt of the AHP grown samples is the forced flow from the annular gap between the baffle and the crucible. An equation in the form of

$$U \approx \frac{R r_c^3}{(r_c^2 - r_b^2)h} \qquad (2)$$

can be used to have an idea about the average velocity of the forced flow (U) in the growth region (melt below baffle). In this equation, R is the growth velocity, r_c is the radius of the crucible, r_b is the radius of the baffle, and h is the melt height between the baffle and the s/l interface. This equation shows that the strength of the flow increases with decreasing the melt height, increasing the growth velocity, and increasing the radius of the crucible. This equation uses the flow rate in the annular gap between the crucible and baffle, since the average velocity of the fluid flow over the s/l interface is determined by this flow rate and not directly by the growth velocity, R. The value of the average velocity of the fluid flow over the s/l interface for each AHP sample is given in Table 1. With a lower growth velocity, of course, influence of the forced flow is lowered.

(a) B12-40-2

(b) B12-40-2

(c) B12-50-075

(d) B12-50-075

(e) AHP12-10-2

(f) AHP12-10-2

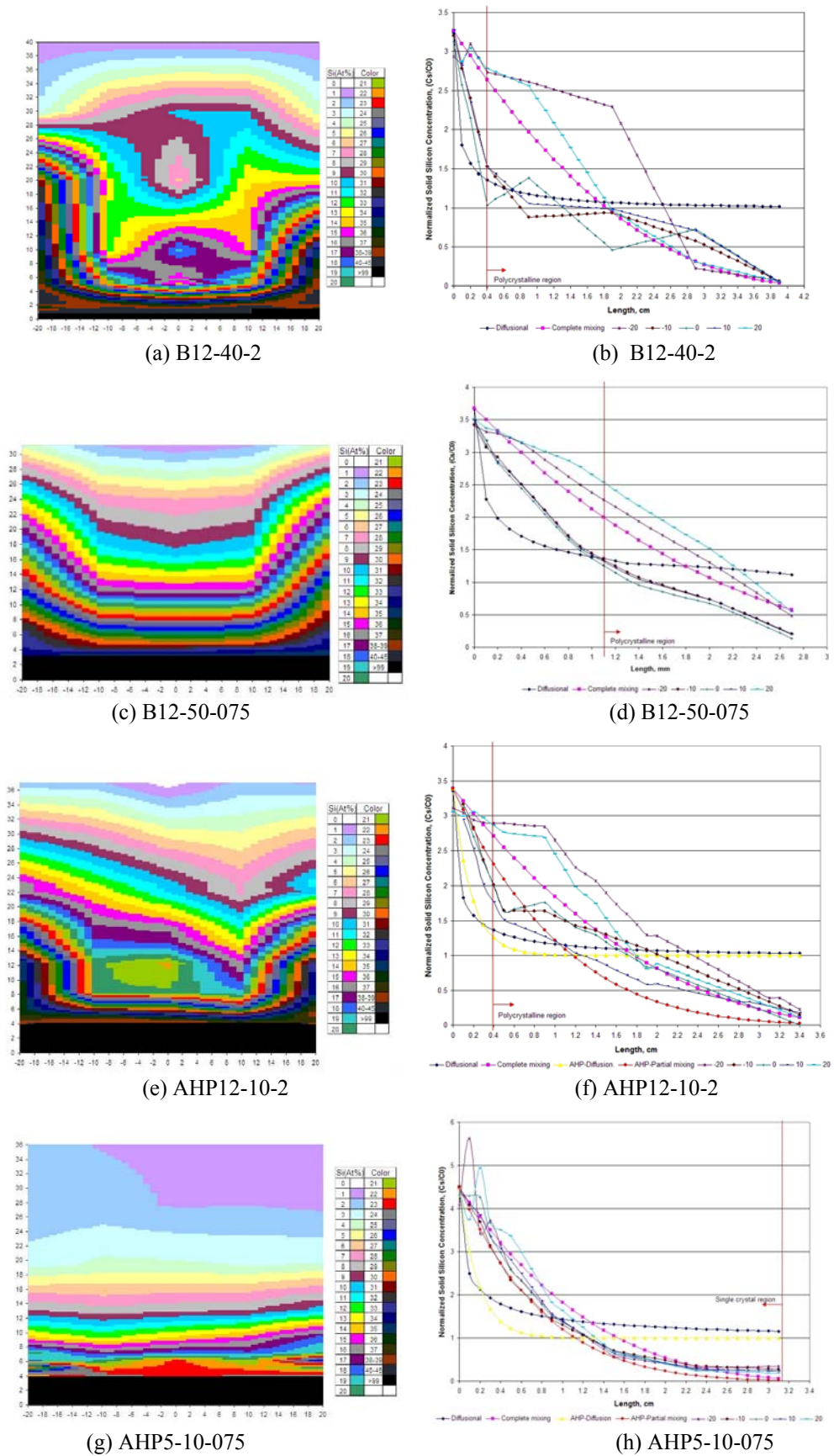(g) AHP5-10-075

(h) AHP5-10-075

Fig. 4 Isoconcentration maps for (a) B12-40-2, (c) B12-50-075, (e) AHP12-10-2, (g) AHP5-10-075 and axial solute concentration profiles for (b) B12-40-2, (d) B12-50-075, (f) AHP12-10-2, (h) AHP5-10-075.

The axial solute concentration profiles for the grown crystals along with the theoretical solute distribution plots for the pure diffusional solute transport mode [19] and complete mixing mode [20] are shown in Figure 4. Figure 4(b), (d), (f), and (h) show that the solute transport mode for all samples is close to the complete mixing radially at the edges. However, towards the center, the mode is diffusional for B12-40-2, mixing for AHP5-10-075, and intermediate for B12-50-075 and AHP12-10-2. All samples have been grown in graphite crucibles. As the crucible has been lowered relative to a stationary furnace, heat loss from the sides has accelerated solidification there, but central region still has stayed molten. Therefore, sides of the crystals solidified from a Si-rich melt and interior regions have solidified from a Si-deficient melt. This, aided by the natural convection, led to a large concavity in VB grown crystals, see Table 1 for curvature depth. A hump in the middle of B12-40-2 is due to solute transport to central region by the convection. When the isoconcentration maps for B12-40-2 (Fig. 4a) and B12-50-075 (Fig. 4c) are investigated comparatively, it is seen that the latter shows a less interface curvature depth. That is because a slow growth velocity allows for homogenization of the melt, minimizing effect of segregation on the melting temperature. During a slow solidification experiment, time for solidification is longer than the time for mixing, so the concentration differences can even out. The homogenization effect of the slow growth velocity is seen better when the two AHP samples are compared. The lower velocity sample, AHP5-10-075 in Fig.4g, shows almost a flat interface with a curvature depth value of only 2 mm. Note that this sample has less initial solute content, as well. Of course, influence of a reduced buoyancy can be seen by comparing isoconcentration maps in Fig. 4a (B12-40-2) and 4e (AHP12-10-2); for same concentration and growth velocity, a lower melt height produces less curvature depth.

The measured single crystal length for each crystal is presented in Table 1. The effects of the growth velocity and initial silicon concentration on the single crystal length can be easily observed from these values; single crystal length of the crystals grown with lower pulling velocity indicates that reducing the growth velocity significantly enhances the interface stability. Another trend which can be seen in the single crystallinity results is the effect of the initial silicon concentration. The samples with the lower initial solute concentration have a longer single crystal region. In fact, the both trends can be summarized into that a flat interface leads to high s/l interface stability since a flat interface has a minimal radial segregation. Three models, constitutional supercooling (CS) [21], Mullin-Sekerka's (MS) perturbation theory [22], and AHP back-diffusion model [23], have been used to investigate the interface stability in crystals grown in this study. The CS and MS models are developed for crystal growth with pure diffusional mixing mode and having constant growth velocity whereas the AHP back-diffusion model considers both diffusional and convectional mixing effects. The CS has a closer estimation than the MS to the experimental

results, but still their stability predictions are far away from the experimental results. In fact, one should not expect these equations to predict the instability in this case since both of them are derived for the pure diffusional systems under the steady state growth conditions. However, the solute transportation in the samples is partial mixing [23] and the growth is not in the steady state condition. Hence, the AHP back-diffusion model is used to predict the interface stability. This model is applicable to the partial mixing and transient cases. However, only the AHP grown crystals are used in the stability analysis since this model is developed for the AHP method. Results of this model are shown in Tab. 1. The AHP back-diffusion predictions are in a very good agreement with the experimental outcomes.

4. Conclusions

Germanium-silicon crystals having 40 mm diameter and up to 50 mm length were grown by the Axial Heat Processing (AHP) and Vertical Bridgman (VB) techniques. Crystals with two different initial concentrations (~ 5 and 12 at. %) were grown with two different pulling velocities (2 mm/h and 0.75 mm/h). A submerged baffle in the AHP method reduced the radial segregation. In addition, the initial solute concentration, pulling velocity, and melt height notably altered the solute redistribution behavior. A flat interface resulted when the radial segregation was minimized by a reduction in the melt height, initial solute content, and growth velocity. Furthermore, a flat interface enhanced the interface stability. Lastly, recently developed AHP-back diffusion model predicted interface stability successfully.

References

[1] E. Kasper, Applied Surface Science, **254**,6158 (2008).
[2] D.J. Paul, Physics World, **13**, 27 (2000).
[3] C.B. Vining, Silicon Germanium, in: D.M. Rowe (Ed.), CRC Handbook of Thermoelectrics, Ch. 28, CRC Press, London, 1995.
[4] C. Wood, Materials for thermoelectric energy conversion, Reports on Progress in Physics **51**, 459 (1988).
[5] J. Schilz, V. N. Romanenko, Journal of Materials Science: Materials in Electronics, **6**, 265 (1995).
[6] V. D., Golyshev, M.A.,Gonik, Russian Patent, Application #4810464(February 1990), Publication #1800854, June 1996.

[7] A. Ostrogorsky, US Patent, Application #397741 (August, 1989), Publication #5047113, September 1991.

[8] V. D. Golyshev, M. A. Gonik, V. B. Tsvetovskii, Instruments and Experimental Techniques **41**, 735 (1998).

[9] V.D. Golyshev, M. A. Gonik, V. B. Tsvetovskii, Journal of Crystal Growth, **198**, 501 (1999).

[10] A. Ostrogorsky, Measurement Science and Technology, **1**, 463 (1990).

[11] C. Marin, A. Ostrogorsky, Journal of Crystal Growth, **211**, 378 (2000).

[12] E. Balikci, A. Deal, R. Abbaschian, The Journal of Crystal Growth, **262**, 581 (2004).

[13] E. Balikci, A. Deal, R, Abbaschian, et al., Journal of Crystal Growth and Design, **4**, 377 (2004).

[14] E. Balikci, A. Deal, R. Abbaschian, The Journal of Crystal Growth, **271**, 37 (2004).

[15] S.V. Bykova, V.D. Golyshev, M.A. Gonik, et al., The Journal of Crystal Growth, **275**, 229 (2005).

[16] A. Deal, E. Balikci, R. Abbaschian, Metallurgical and Materials Transactions A, **38A**, 100 (2007).

[17] A. Dario, H.O. Sicim, E. Balikci, Journal of Crystal Growth, **318**, 1057 (2011).

[18] A. Dario, H.O. Sicim, E. Balikci, Journal of Crystal Growth, **351**, 1 (2012).

[19] V. G. Smith, W. A. Tiller, J. W. Rutter, Canadian Journal of Physics **33**, 723 (1955).

[20] Scheil, E., Retrogate saturation curves, Zeitschrift für Metallkunde, **34**, 70 (1942).

[21] W.A.Tiller, K.A.Jackson, J. W. Rutter, B. Chalmers, Acta Metallurgica, **1**, 428 (1953).

[22] W. W.Mullins, R. F. Sekerka, Journal of Applied Physics, **35**, 444 (1964).

[23] A. Dario, H. O. Sicim, E. Balikci, Journal of Crystal Growth, **337**, 65 (2011).

[*]Corresponding author: ercan.balikci@boun.edu.tr